Imbalance between vertical nitrate flux and nitrate assimilation on a continental shelf: Implications of nitrification

Takuhei Shiozaki,[1] Ken Furuya,[1] Hiroyuki Kurotori,[1,2] Taketoshi Kodama,[1] Shigenobu Takeda,[1,3] Takahiro Endoh,[4] Yutaka Yoshikawa,[4] Joji Ishizaka,[5,6] and Takeshi Matsuno[4]

Received 30 December 2010; revised 28 July 2011; accepted 5 August 2011; published 26 October 2011.

[1] The nitrate assimilation rate and diapycnal nitrate flux were simultaneously determined on the continental shelf of the East China Sea (ECS). Further, the archaeal *amoA* gene was quantified to examine the potential distribution of nitrification activity. Nitrate assimilation rates and distribution of the archaeal *amoA* gene were also investigated in the Philippine Sea and in the Kuroshio Current. At all the stations, while the surface nitrate was depleted (<0.1 μM), active nitrate assimilation was observed with mean rates of 1400, 270, and 96 μmolN m^{-2} d^{-1} in the ECS, the Philippine Sea, and the Kuroshio Current, respectively. Archaeal *amoA* was observed at shallower light depths, namely at or above 10% light depth, in the ECS than in other regions, suggesting that nitrification occurred within the euphotic zone in the ECS, especially on the shelf. Moreover, a station on the continental shelf of the ECS exhibited a considerable discrepancy between the nitrate assimilation rate (1500 μmolN m^{-2} d^{-1}) and vertical nitrate flux (98 μmolN m^{-2} d^{-1}). Here, $6.7 \pm 3.1 \times 10^3$ and $2.5 \pm 0.7 \times 10^5$ copies mL^{-1} of archaeal *amoA* were detected at 10% and 1% light depths relative to the surface, respectively. Thus nitrification within the euphotic zone would be attributed at least in part to the observed discrepancy between nitrate assimilation and vertical flux. These observations imply that the assumption of a direct relationship between new production, export production, and measured nitrate assimilation is misplaced, particularly regarding the continental shelf of the ECS.

Citation: Shiozaki, T., K. Furuya, H. Kurotori, T. Kodama, S. Takeda, T. Endoh, Y. Yoshikawa, J. Ishizaka, and T. Matsuno (2011), Imbalance between vertical nitrate flux and nitrate assimilation on a continental shelf: Implications of nitrification, *J. Geophys. Res.*, *116*, C10031, doi:10.1029/2010JC006934.

1. Introduction

[2] New production is defined as primary production stimulated by newly available nitrogen [*Dugdale and Goering*, 1967]. The ratio of new production to total production is called the *f* ratio, which indicates the fraction of sinking (export) flux to total production [*Eppley and Peterson*, 1979].

[3] Nitrate is the most abundant form of inorganic nitrogen compounds in oceans [*Wada and Hattori*, 1991]. The bioavailable nitrogen introduced into the euphotic zone from the deep is primarily in the form of nitrate; hence, it has been considered that the primary production sustained by nitrate is new production, and nitrate-based new production can be estimated by the $^{15}NO_3^-$ assimilation rate [*Dugdale and Goering*, 1967]. In a previous study, *Lewis et al.* [1986] simultaneously determined the nitrate assimilation rate and upward nitrate flux in the oligotrophic Atlantic Ocean and demonstrated that there were no significant differences. On the basis of on these theoretical and experimental backgrounds, $^{15}NO_3^-$ assimilation measurements have been applied as the standard method for estimating nitrate-based new production from the time the Joint Global Ocean Flux Study (JGOFS) was introduced; that is, from 1988 to 2003 [*United Nations Educational, Scientific and Cultural Organization* (*UNESCO*), 1994]. However, recent studies have shown that the generation of nitrate by nitrification near the surface is not negligible and, furthermore, that the nitrate assimilation method overestimates nitrate-based new production owing to the inclusion of regenerated nitrate within the euphotic zone [*Dore and Karl*, 1996; *Yool et al.*, 2007; *Clark et al.*, 2008]. Recent molecular biological studies have revealed a new pathway of ammonia oxidation through the domain archaea; moreover, ammonia-oxidizing archaea is ubiquitous in the ocean, and it is considerably more abundant than another nitrifier, ammonia-oxidizing bacteria [*Francis*

[1]Department of Aquatic Bioscience, Graduate School of Agricultural and Life Sciences, University of Tokyo, Tokyo, Japan.
[2]Now at Riso Co. Ltd., Tokyo, Japan.
[3]Now at Graduate School of Fisheries Science and Environmental Studies, Nagasaki University, Nagasaki, Japan.
[4]Research Institute for Applied Mechanics, Kyushu University, Fukuoka, Japan.
[5]Faculty of Fisheries, Nagasaki University, Nagasaki, Japan.
[6]Now at Hydrospheric Atmospheric Research Center, Nagoya University, Nagoya, Japan.

0148-0227/11/2010JC006934

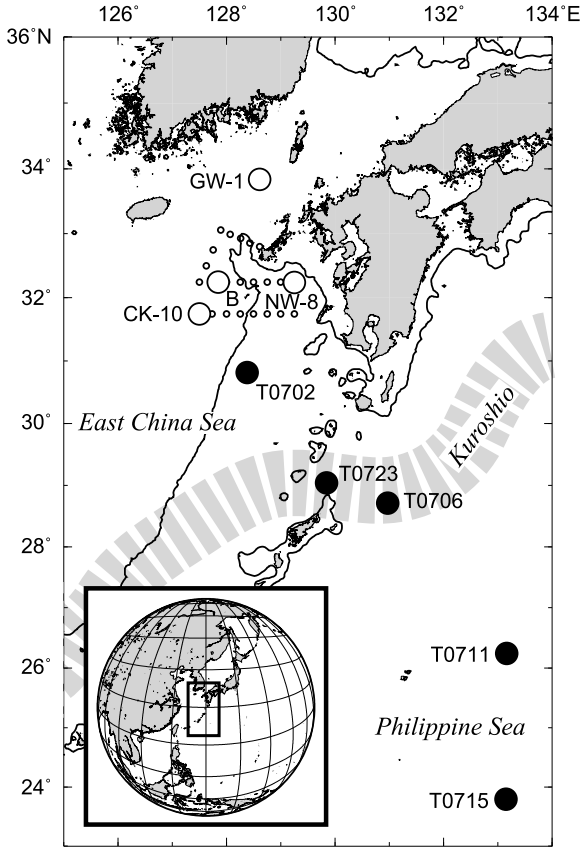

Figure 1. Sampling stations in the northwestern East China Sea and the Philippine Sea during the *Nagasaki-maru* 242 (open circles) and the KT-07-22 (solid circles) cruises. Big circles indicate the major stations, and small circles are the stations where samples for nutrients and chlorophyll *a* only were taken. The shaded dashed line represents the path of the Kuroshio (see text). Solid lines denote 200 m isobaths.

et al., 2005; *Wuchter et al.*, 2006; *Mincer et al.*, 2007; *Beman et al.*, 2008; *Galand et al.*, 2009]. Ammonia oxidation is the first step of nitrification in which ammonia is oxidized to nitrate with two reactions ($NH_4^+ \rightarrow NO_2^- \rightarrow NO_3^-$) mediated by microbes. *Beman et al.* [2008] showed a strongly positive correlation between ammonia oxidation rates and archaeal *amoA* gene copies ($r^2 = 0.90$, $p < 0.001$) in the Gulf of California, suggesting that the presence of the *amoA* gene indicates nitrification.

[4] In theory, at steady state, or over sufficiently long time spans, new production should be balanced by export production [*Eppley and Peterson*, 1979]. *Chen* [2003] reviewed new and export production in continental shelf waters in the East China Sea (ECS) and contrasted it with results from the open ocean. He found that nitrate-based new production on the shelf is considerably higher than values expected from export production. To explain this discrepancy, *Chen* [2003] hypothesized that nitrogen remineralized in the bottom sediment easily returns to the euphotic zone on the continental shelf. However, recent progress in the study of nitrogen processes suggests that this discrepancy can be attributed to nitrification activity even in the euphotic zone [*Dore and Karl*, 1996; *Yool et al.*, 2007; *Clark et al.*, 2008]. Although nitrate assimilation in the ECS has long been studied [*Chen et al.*, 1999, 2001; *Kanda et al.*, 2003], few studies on nitrification exist.

[5] This is the first report on the simultaneous determination of the nitrate assimilation rate and diapycnal nitrate flux on a continental shelf. The present study used the Michaelis-Menten kinetics approach to estimate the nitrate assimilation rate [*Kanda et al.*, 2003; *Shiozaki et al.*, 2009]. $^{15}NO_3^-$ is generally added at a low concentration of 30–100 nM in nitrate assimilation experiments [*Lipschultz*, 2008]. However, even with a low concentration of $^{15}NO_3^-$, the nitrate assimilation rate is overestimated in the oligotrophic ocean, because the added $^{15}NO_3^-$ concentration excess tracer level is <10% of the ambient concentration [*Lipschultz*, 2008]. In contrast, the Michaelis-Menten kinetics approach corrects the overestimation caused by the excessive use of ^{15}N; hence, this approach is considered more accurate than the conventional method [*Harrison et al.*, 1996; *Kanda et al.*, 2003].

2. Materials and Methods

[6] Observations and sampling were conducted on board the T/V *Nagasaki-maru* 242 (19–28 July 2007) and R/V *Tansei-maru* KT-07-22 (5–13 September 2007) cruises in the ECS, the Kuroshio, and the Philippine Sea (Figure 1). The ECS has a large shelf area occupying approximately 70% of the total area; further, its euphotic zone, in which nitrate is depleted in the summer, occasionally receives large nutrient supplies by riverine inputs near the coast, vertical mixing, and atmospheric deposition [*Chen*, 2003]. In contrast, the Philippine Sea has fewer allochthonous nitrogen inputs than the ECS, suggesting that there is little primary production in the former [*Shiozaki et al.*, 2010].

[7] Temperature and salinity profiles down to 200 m were obtained on *Nagasaki-maru* and *Tansei-maru* using a SBE 911plus (Sea Bird Electronics, Inc.) conductivity, temperature, and depth profiler (CTD) and an integrated CTD (ICTD) (Falmouth Scientific, Inc.), respectively. This depth range adequately sampled the euphotic zone. Water samples for nutrients and chlorophyll *a* were obtained at between 8 and 16 depths within the upper 200 m using an acid-cleaned bucket and Niskin-X bottles, while the samples for incubation experiments were taken at four depths corresponding to 100, 25, 10, and 1% of the surface light intensity. The sampling depths for the incubation experiments were selected on the basis of the measured vertical light profile; these profiles, in turn, were determined using PRR-800 (Biospherical Instruments, Inc.) during the KT-07-22 cruise and estimated from the empirical relationship between the surface chlorophyll *a* concentration and the attenuation coefficient of downwelling irradiance [*Siswanto et al.*, 2005] during the *Nagasaki-maru* 242 cruise.

2.1. Nutrients and Chlorophyll *a*

[8] Samples for nutrient analysis were collected in duplicate acid-cleaned polypropylene bottles (50 or 100 mL) and were kept frozen until analyses were conducted on land. The concentrations of nitrate, nitrite, and soluble reactive phosphorus (SRP) were first examined by a conventional colorimetric method. When the nutrient concentrations at the stations where the nitrate assimilation and flux were determined (major stations) were below 0.1 μM, they were analyzed using a supersensitive colorimetric system (detection

limit: 3 nM) comprising an AutoAnalyzer II (Technicon) connected to a liquid waveguide capillary cell (LWCC, World Precision Instruments, Inc.) [*Hashihama et al.*, 2009]. When the initial nitrate concentration for the nitrate assimilation experiment was below the detection limit even when the supersensitive colorimetric system was used, the nitrate concentration was assumed to be within the detection limit of 3 nM. The nitracline depth was defined as the depth at which the nitrate concentration was greater than 1 μM.

[9] Samples containing chlorophyll *a* were filtered using 25 mm Whatman GF/F filters, and the chlorophyll *a* concentrations were determined using a Turner Designs 10 AU fluorometer after extraction with *N*, *N*-dimethylformamide [*Suzuki and Ishimaru*, 1990].

2.2. Vertical Eddy Diffusivity and Diapycnal Nitrate Flux

[10] During the *Nagasaki-maru* 242 cruise, the turbulent velocity shear was measured to a depth of 75 m using a TurboMAP5 free-falling microstructure profiler (Alec Electric Co.) in order to estimate the vertical eddy diffusivity at four stations (CK-10, GW-1, B, and NW-8). At station B, the turbulent velocity shear was measured almost every hour for 24 h by tracking a drifting global positioning system (GPS) buoy. The data analysis procedure for TurboMAP5 has been described elsewhere in detail [*Matsuno et al.*, 2005, 2006]. The vertical eddy diffusivity K_z ($m^2\ s^{-1}$) was calculated using equation (1) [*Osborn*, 1980] as follows:

$$K_z = \lambda\varepsilon/N^2 \tag{1}$$

Here, ε ($W\ kg^{-1}$) and N (s^{-1}) are the turbulent kinetic energy dissipation rate and the Brunt-Väisälä frequency obtained by the TurboMAP5 measurements, respectively, while λ (dimensionless) was assumed to be constant at 0.2 [*Matsuno et al.*, 2005, 2006].

[11] The turbulent nitrate flux of F ($\mu molN\ m^{-2}\ d^{-1}$) is calculated using K_z and the nitrate gradient ($\partial NO_3^-/\partial z$; $\mu mol\ m^{-4}$) at the nitracline on the basis of the Fickian diffusion theory (equation (2)).

$$F = K_z\,\partial NO_3{}^-/\partial z \tag{2}$$

The vertical profile of ε included the tidal effect [*Matsuno et al.*, 2005]. Therefore, tidal mixing is considered in estimates of turbulent nitrate flux. Daily turbulent nitrate flux was calculated with the assumption that both measured K_z and nitrate gradient were constant.

[12] Since ε at depths shallower than 20 m is relatively high due to wind-induced diffusivity [*Matsuno et al.*, 2006], the K_z used for the calculation of the turbulent nitrate flux was the average K_z below 20 m. The 95% confidence intervals (hereafter 95% CI) for K_z and for the turbulent nitrate flux were computed by the bootstrap method [*Efron and Gong*, 1983; *Carr et al.*, 1995].

2.3. Nitrate Assimilation Rate

[13] Nitrate assimilation experiments were conducted at station B during the *Nagasaki-maru* 242 cruise and at all stations during the KT-07-22 cruise. All the experiments were performed in nitrate-depleted surface waters (<0.1 μM), and the assimilation rates were calculated using the Michaelis-Menten kinetics approach to correct the overestimation caused by the excessive use of ^{15}N tracer [*Kanda et al.*, 2003; *Shiozaki et al.*, 2009]. The samples collected (4.5 L) for estimating the initial ^{15}N enrichment of particulate organic nitrogen were filtered immediately at the beginning of the incubation. The samples for incubation were collected in four acid-cleaned 2 L polycarbonate bottles, and ^{15}N-labeled nitrate (99.8 atom% ^{15}N; Shoko) was spiked into each bottle to give final tracer concentrations of 10, 100, 300, and 2000 nM. The samples were subsequently wrapped in neutral-density screens to adjust each light level and then incubated during the daytime in an on-deck incubator cooled by flowing surface seawater. The experiments were terminated within 3 h. At stations B, T0715, and T0723, the incubations were performed during both daytime and nighttime. Detailed procedures for the pretreatment and analysis have been described elsewhere [*Shiozaki et al.*, 2009].

[14] Nitrate assimilation rates ρ_n ($nmolN\ l^{-1}\ h^{-1}$) at ^{15}N tracer concentration S_n (nM) were fitted to equation (3) to estimate the maximum saturation rate ρ_{max} ($nmolN\ l^{-1}\ h^{-1}$) and the half-saturation constant K_S (nM) by the least squares method:

$$\rho_n = \frac{\rho_{max} \times (S + S_n)}{K_S + (S + S_n)} \tag{3}$$

where S (nM) is the ambient nitrate concentration. Then, in situ nitrate assimilation rates (ρ_k; $nmolN\ l^{-1}\ h^{-1}$) were calculated from equation (4) using estimated values of ρ_{max} and K_S.

$$\rho_k = \frac{\rho_{max} \times S}{K_S + S} \tag{4}$$

[15] At stations B and T0702 where nitrate concentrations were over 3 μM at 1% light depth, the samples were spiked with only 300 nM of the tracer, and the nitrate assimilation rates ρ_n were regarded as ρ_k. Depth-integrated nitrate assimilation was calculated by trapezoidal integration.

2.4. DNA Collection, Extraction, Polymerase Chain Reaction, Cloning, and Sequencing

[16] The samples for DNA analysis were collected in a 1 L polypropylene bottle at the stations where incubation experiments were conducted during the cruises. The samples were gently filtered (<100 mmHg) onto 47 mm diameter, 0.2 μm pore size Nuclepore filters. The filters were placed in 2 mL centrifuge tubes containing 500 μl of Tris-EDTA (TE), and were stored in liquid nitrogen for ashore analysis.

[17] DNA was extracted from filters following the protocol described by *Tillett and Neilan* [2000]. Sodium dodecyl sulfate (SDS, 50 μl, 20% w/v stock) and 460 μl of xanthogenate buffer (2% potassium ethyl xanthogenate; 200 mM Tris-HCl, pH: 7.4; 40 mM EDTA, pH: 8.0; 1.6 M ammonium acetate; 0.2 mg mL^{-1} RNAseA) were added to centrifuge tubes containing filters and 500 μl of TE buffer and then gently mixed. The filters were incubated at 60°C for 120 min and placed on ice for 10 min. The filters were then centrifuged at 14,000 × g for 15 min at room temperature. The supernatant was transferred to new 2 mL centrifuge tubes containing

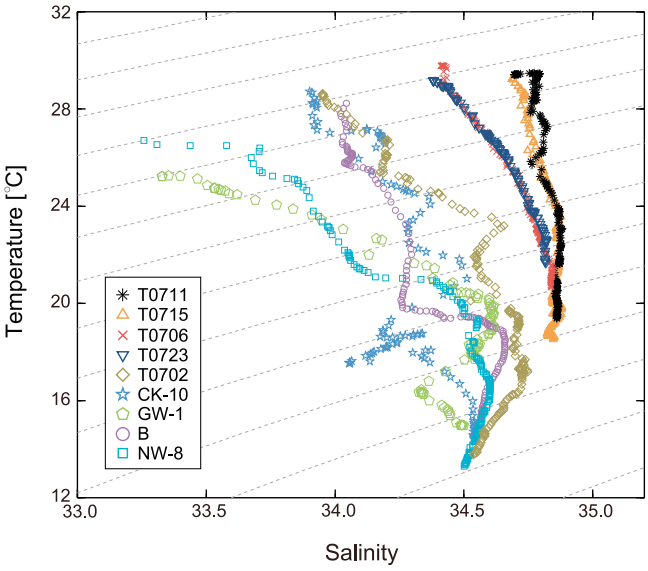

Figure 2. Temperature-salinity (T-S) diagram of the upper 200 m water columns at the major stations.

900 μl of 99% isopropanol and placed at −20°C overnight. DNA was precipitated by centrifugation at 14,000 × g for 20 min at room temperature, and the DNA pellet was washed with cold 70% ethanol and centrifuged again for 10 min at 4°C. This ethanol wash was performed twice. The supernatant was then removed, and the samples were dried and resuspended in 100 μl of 1 × TE. The samples were stored at −20°C until analysis.

[18] Archaeal *amoA* gene fragments were amplified using the PCR primers Arch-amoAF and Arch-amoAR, which *Francis et al.* [2005] described. The PCR products (10 μl) were analyzed on a 1% agarose gel and purified using a Wizard Plus Minipreps DNA Purification System (Promega). The purified samples were cloned with pGEM®-T Easy Vector Systems (Promega), transformed into *Escherichia coli* DH5α, and then selected by a blue-white selection. The plasmids were purified using a QIAprep Spin Miniprep kit (Qiagen) and sequenced with an ABI3100 (Applied Biosystems). The plasmids with the sequenced gene fragment (DDBJ accession no.: AB576803) were used as the quantitative PCR (qPCR) standard.

2.5. The qPCR Assay

[19] All qPCR assays were run on MiniOpticon (Bio-Rad Laboratories) with the same primers for the quantification of archaeal *amoA*. Twenty microliters of the qPCR mixtures contained 10 μl Power SYBR® Green PCR Master Mix (Applied Biosystems), 0.3 μM of each primer, and 1 μl template DNA. qPCR was performed in triplicate with the parameters given by *Beman et al.* [2008]: 95°C for 4 min, 50 cycles of 30 s at 95°C, 45 s at 53°C, and 60 s at 72°C with a detection step at the end of each cycle. The standard curve ranging from 10 to 10^5 gene copies was prepared for each reaction using plasmids with the target *amoA* insert. The specificity of the qPCR primer was confirmed by the melting curves generated after each assay, and the efficiency of the PCR reaction varied between 81% and 93%, with a mean of 85%.

3. Results

3.1. Hydrographic Conditions, Nutrients, and Chlorophyll *a*

[20] The Kuroshio flowed through stations T0706 and T0723 during the KT-07-22 cruise (http://www1.haiho.milt.go.jp/KANKYO/KAIYO/qdoc/index.html). In Figure 2, the water masses form a distinct cluster on the temperature-salinity (T-S) diagram, and these are referred to as the Kuroshio in the present study. Stations T0711 and T0715 are located in the Philippine Sea. The waters in the Philippine Sea had higher salinity than those in the Kuroshio and are shown separately in the T-S diagram (Figure 2). Finally, the other stations were clustered into one group and hence are referred to hereafter as the ECS. The temperature at the surface ranged from 25.1 to 29.5°C, and the salinity varied between 33.2 and 34.7 (Table 1).

[21] Although nitrate concentrations at the surface were depleted (<0.1 μM) at all stations, there were significant differences among the regions at nanomolar levels (Figure 3a). The nitrate concentration at depths above 50 m in the Philippine Sea and the Kuroshio were <~10 nM, while that in the ECS was always ≥10 nM except at the surface at station T0702. The nitracline depth ranged from 32 to 62 m in the ECS, 159 and 171 m in the Philippine Sea, and 134 m and >200 m in the Kuroshio (Table 1). Furthermore, the nitracline depth in the ECS was significantly shallower than that in the other two regions. The nitrate concentration below the nitracline increased immediately in the ECS, unlike the case in the other two regions. The nitrate gradient at the nitracline ranged from 120 to 240 μmol m^{-4} in the ECS, 17 ± 0.2 (± standard error; hereafter, uncertainties of parameters were described as standard error unless otherwise noted) and 33 ± 1.6 μmol m^{-4} in the Philippine Sea, and 20 ± 3.8 μmol m^{-4} in the Kuroshio (Table 1).

[22] The nitrite concentrations showed vertical maxima at all the major stations (Figure 3b). While the peak was observed below the 1% light depth in the Philippine Sea and the Kuroshio, it was located in the euphotic zone in the ECS. The maxima were significantly higher in the ECS than in the other regions, while those in the Kuroshio were higher than those in the Philippine Sea.

[23] The SRP concentrations at the surface varied between <3 and 32 nM at all the major stations [*Shiozaki et al.*, 2010, Figure 2b]. Similar to the nitrate distribution, the SRP concentration was immediately elevated below the nitracline in the ECS, while the SRP gradient was higher in the ECS than in the Philippine Sea or the Kuroshio (data not shown). However, the upper 50 m of SRP in the ECS did not always exceed the values in the other two regions. The relative abundance of SRP according to the Redfield ratio was higher than the nitrate + nitrite concentrations; hence, phytoplankton were more limited by nitrogenous nutrients in our study regions.

[24] Surface chlorophyll *a* ranged from 0.09 to 0.22 μg l^{-1} at all the major stations, while the depth-integrated chlorophyll *a* varied from 13.0 ± 0.45 to 20.5 mg m^{-2} up to 1% light depth; this implied no significant difference between the

Table 1. Summary of Variables at the Major Stations[a]

Station	Temperature (°C)	Salinity at 5 m Depth	Depth-Integrated Chlorophyll *a* (mg m^{-2})	Bottom Depth (m)	1% Light Depth (m)	Nitracline Depth (m)	Nitrate Gradient at the Nitracline, dNO_3^-/dz (μmol m^{-4})	Vertical Eddy Diffusivity, K_z[b] ($\times 10^{-5}$ m^2 s^{-1})	Vertical NO_3^- Flux[c] (μmolN m^{-2} d^{-1})	Nitrate Assimilation, ρNO_3^- (μmolN m^{-2} d^{-1})
						Philippine Sea				
T0711	29.4	34.7	15.5	5356	126	171	17 ± 0.2	2.2[d] (0.67–4.4)	33 (9.3–68)	290
T0715	29.2	34.7	19.8	2949	128	159	33 ± 1.6	2.2[d] (0.67–4.4)	63 (15–150)	240
						Kuroshio				
T0706	29.8	34.4	20.5	3094	108	>200	-[e]	2.2[d] (0.67–4.4)	-	110
T0723	29.2	34.4	17.4	951	91	134	20 ± 3.8	2.2[d] (0.67–4.4)	38 (2.1–140)	79
						East China Sea				
T0702	28.6	34.0	13.6	626	67	38	120 ± 0.65	2.2[d] (0.67–4.4)	230 (68–470)	1100 (680)[f]
CK-10	29.1	33.9	14.9	133	82	49	200 ± 30	1.8 (0.90–2.9)	310 (55–820)	-
GW-1	25.1	33.2	19.1	106	61	32	240 ± 59	5.7 (1.4–12)	1200 (0–5100)	-
B	28.2 ± 0.07[g]	34.0 ± 0.01[g]	13.0 ± 0.45[g]	149	70	62 ± 2[g]	170 ± 1.9[g]	0.67 (0.36–0.97)	98 (52–150)	1700 (1500)[f]
NW-8	26.4	33.4	17.6	337	65	36	110 ± 12	0.67 (0.43–0.96)	64 (27–120)	-

[a]Chlorophyll *a* and ρNO_3 were integrated from surface to the 1% light depth.
[b]95% confidence interval.
[c]Calculated using equation (2). 95% confidence interval.
[d]Mean (95% confidence interval) of the determined values during Nagasaki-maru 242 cruise.
[e]Data were not available.
[f]Since nitracline was shallower than the 1% light depth, the ρNO_3 was calculated from surface to the nitracline (see text).
[g]Mean ± standard error during the 24-hours-time-series observation.

regions (Figure 3c and Table 1). However, the maximum concentration of chlorophyll *a* in the ECS surpassed the concentrations in the other two regions except for station T0706. Subsurface chlorophyll *a* maximum (SCM) developed at all the major stations and was generally located at the 1% light depth. Although SCM in the Philippine Sea and the Kuroshio was observed above the nitracline, that in the ECS was located around or below the nitracline.

3.2. Vertical Eddy Diffusivity and Diapycnal Nitrate Flux

[25] The magnitude of ε varied vertically between $O(10^{-10})$ and $O(10^{-7})$ m^2 s^{-3}, and there were no notable differences among all four stations (only the results from station B are shown in Figure 4). The vertical profiles of K_z below 20 m ranged from $O(10^{-7})$ to $O(10^{-4})$ at all the stations. Since ε varied over a relatively wider range than N^2, the K_z profiles showed a structure similar to that of ε. The average K_z below 20 m ranged from 0.67 to 5.7 $\times$ 10^{-5} m^2 s^{-1} with a mean of 2.2 $\times$ 10^{-5} (0.67–4.4 $\times$ 10^{-5}, 95% CI) m^2 s^{-1} at all the stations, while the diapycnal nitrate flux estimated by equation (2) varied from 64 (27–120, 95% CI) to 1200 (0–5100) μmolN m^{-2} d^{-1} in the ECS (Table 1).

3.3. Nitrate Assimilation Rate

[26] The nitrate assimilation rate was typically higher in the daytime than at night, and the difference between the daytime and nighttime rates varied from region to region. The depth-integrated nitrate assimilation rates at night down to the 1% light depth were 45, 16, and 18% of the daytime rates in the ECS (station B), the Philippine Sea (station T0715), and the Kuroshio (station T0723), respectively. Since the light:dark ratio was approximately 12:12 in the present study, the daily assimilation rate ρ_{daily} (nmolN l^{-1} d^{-1}) was calculated by weighted summing of the daytime rate, ρ_{day} (nmolN l^{-1} h^{-1}), and nighttime rate, ρ_{night} (nmolN l^{-1} h^{-1}), in each region [*Peña et al.*, 1992; *Aufdenkampe et al.*, 2002].

$$\rho_{daily} = 12 \int \rho_{day} + 12 \int \rho_{night} \tag{5}$$

[27] Depth-integrated rates of nitrate assimilation were calculated above the 1% light depth at all the stations. However, since the nitracline was shallower than the 1% light depth in the ECS (Table 1), the nitrate assimilation rate was integrated from the surface to the top of the nitracline for comparison with the vertical nitrate flux estimated by equation (2). The rate at the top of the nitracline was computed by linear interpolation from the neighboring light depths.

[28] The average values of the depth-integrated assimilation rates above the 1% light depth were 1400, 270, and 96 μmolN m^{-2} d^{-1} in the ECS, Philippine Sea, and Kuroshio, respectively. That above the top of the nitracline was 1100 μmolN m^{-2} d^{-1} in the ECS. Obviously, the rates were considerably higher in the ECS than in the other regions. At station B in the ECS, the depth-integrated rate of 1700 μmolN m^{-2} d^{-1} above the 1% light depth (1500 μmolN m^{-2} d^{-1} above the top of the nitracline) was one order of magnitude higher than the diapycnal nitrate flux of 98 (52–150, 95% CI) μmolN m^{-2} d^{-1}, which was determined at the same time. The vertical maximum of the nitrate assimilation

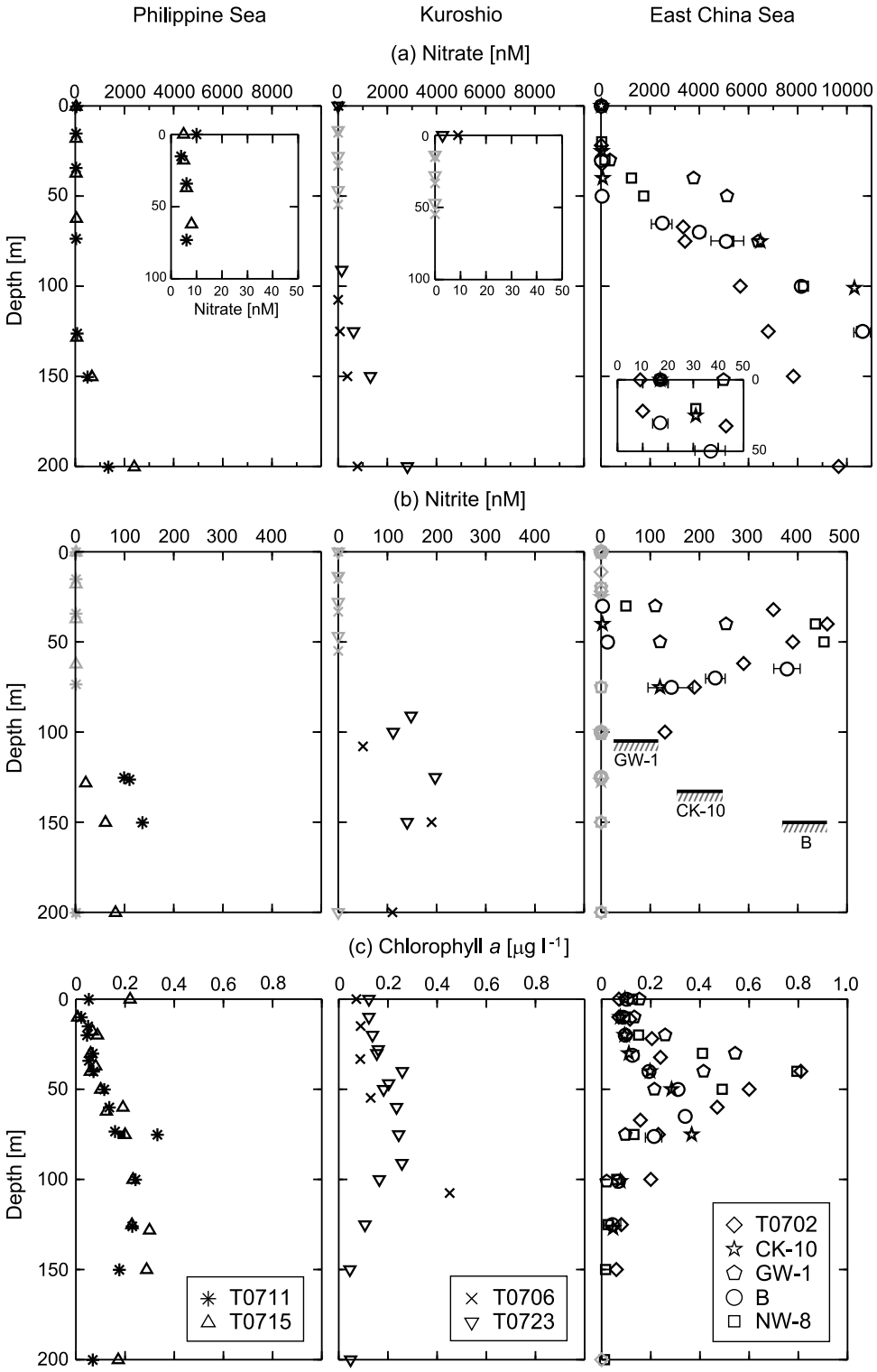

Figure 3. Vertical profiles of (a) nitrate (nM), (b) nitrite (nM), and (c) chlorophyll *a* (μg l^{-1}) at the major stations in the Philippine Sea, the Kuroshio, and the East China Sea, respectively. Nitrate concentrations above 100 or 50 m are scaled up in the inset. Gray symbols indicate below the analytical detection limits. Error bars denote standard errors during the 24 h time series observations. Bottom depths were drawn in the East China Sea.

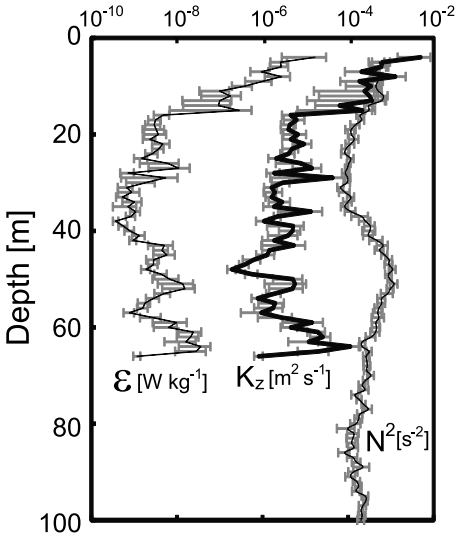

Figure 4. Vertical profiles of ε (W kg^{-1}), K_z (m^2 s^{-1}), and N^2 (s^{-2}) at station B. Error bars represent the standard errors during the 24 h time series observation.

occurred at the surface and at 25% light depth in the Philippine Sea and at the surface in the ECS and Kuroshio (Figure 5). At all the stations except stations B and T0706, the assimilation rate was higher at the 1% light depth than at the 10% light depth.

3.4. Archaeal *amoA* Copy Numbers

[29] In general, archaeal *amoA* abundance showed vertical maxima at or under 1% light depth and was undetected at the surface, while the distributions varied significantly among the three regions (Figure 6). In the ECS, there were $6.7 \pm 3.1 \times 10^3$ and $2.5 \pm 0.7 \times 10^5$ copies mL^{-1} of archaeal *amoA* at station B at 10% and 1% light depths, respectively. Although the highest abundance of archaeal *amoA* in the euphotic zone at station T0702 was lower than that at station B, archaeal *amoA* was detected above the 10% light depth (30 m). The vertical profile of archaeal *amoA* at station T0702 indicated two peaks, at 100 and 200 m. Archaeal *amoA* was observed at around 1% light depth in the Philippine Sea, and it increased with depth. In the Kuroshio, although archaeal *amoA* was absent in the euphotic zone, it was detected at depths of deeper than 100 m and the maxima were one order of magnitude higher than those in the Philippine Sea.

4. Discussion

4.1. Spatial Variations in Nitrate Assimilation Rates and Nitrate Upward Flux

[30] The present study demonstrated a distinct regional variability in nitrate assimilation rates among the three oceanographic regions: the ECS, the Philippine Sea, and the Kuroshio. *Kanda et al.* [2003] examined seasonal variations in nitrate assimilation rates above 1% light depth in the ECS and the Kuroshio along a transect from the Changjiang River mouth to the Okinawa Trough. They reported that the rates on the continental shelf (280–1700 μmolN m^{-2} d^{-1}) were significantly higher than those on the shelf break, including the Kuroshio, in summer (100–390 μmolN m^{-2} d^{-1}). In the present study, the nitrate assimilation rate above the 1% light depth at station B located on the shelf (1700 μmolN m^{-2} d^{-1}) was higher than that at station T0702 on the edge of the shelf in the ECS (1100 μmolN m^{-2} d^{-1}); further, the rates in the Kuroshio were considerably lower than those in the ECS. These regional trends were consistent with the results of *Kanda et al.* [2003]. In addition, the mean nitrate assimilation rate in the Philippine Sea (270 μmol N m^{-2} d^{-1}) was within the range of the results of a previous study conducted in the western tropical and subtropical North Pacific [*Shiozaki et al.*, 2009].

[31] Conventionally, these regional variations in nitrate assimilation can be attributed to the differences in vertical nitrate fluxes [*King and Devol*, 1979; *Chen*, 2003]. *Matsuno*

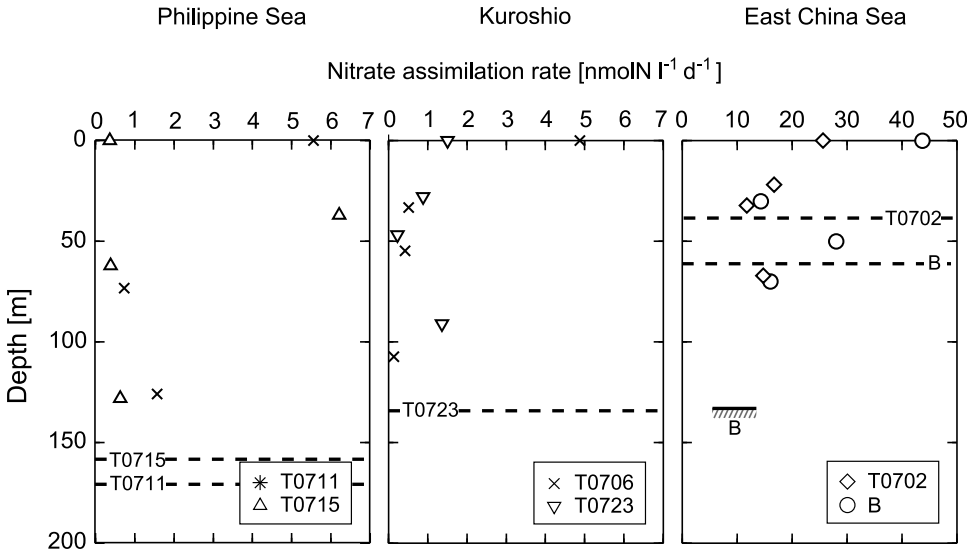

Figure 5. Vertical profiles of nitrate assimilation (nmolN l^{-1} d^{-1}) in the Philippine Sea, the Kuroshio, and the East China Sea. Dashed lines indicate the nitracline.

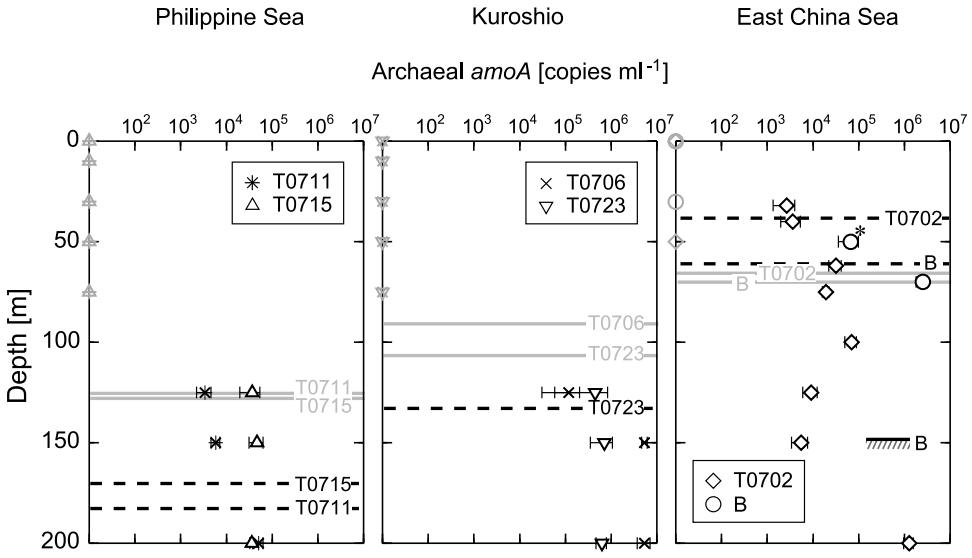

Figure 6. Vertical profiles of archaeal *amoA* gene copy number (copies per milliliter) in the Philippine Sea, the Kuroshio, and the East China Sea. Gray symbols indicate below the analytical detection limits. Error bars denote standard errors of triplicate analyses. Dashed and gray lines represent the nitracline and the 1% light depth, respectively. Asterisks denote 10% light depth.

et al. [2005] reported that the vertical eddy diffusivity on and off the shelf rarely exceeded O (10^{-4}) except near the surface and floor, and decreased to O (10^{-5}–10^{-6}) in the water column. Our estimations were similar to those of the reported distribution. Moreover, we applied the average K_z of 2.2 (0.67–4.4 × 10^{-5}, 95% CI) × 10^{-5} m^2 s^{-1} to station T0702 in the ECS and to the stations in the other two regions. Vertical nitrate flux in the ECS ranging from 64 (27–120, 95% CI) to 1200 (0–5100) μmolN m^{-2} d^{-1} tended to be higher than those in the Philippine Sea (33 (9.3–68) and 63 (15–150) μmolN m^{-2} d^{-1}) and the Kuroshio (38 (2.1–140) μmolN m^{-2} d^{-1}; see Table 1). These results support the view in the previous study [*Chen*, 2003] that vertical nitrate flux is higher on or near the continental shelf than in the open ocean.

4.2. Distribution of Archaeal *amoA* in the ECS and Its Adjacent Waters

[32] The maximum depth of archaeal *amoA* and its abundance had significant regional variations, as mentioned in section 3. Although a few reports have described the vertical distributions of archaeal *amoA* in the euphotic zone, archaeal *amoA* is recognized to have a maximum near the bottom of the euphotic zone and to have little presence at the surface [*Mincer et al.*, 2007; *Beman et al.*, 2008]. In the present study, the vertical profiles were similar to those in the previous studies in all regions. The highest abundance (5.4 ± 0.7 × 10^5 copies mL^{-1}) in the Kuroshio was greater than that in the North Pacific subtropical gyre (~1 × 10^4 copies mL^{-1}) or that in the coastal region (~6 × 10^4 copies mL^{-1}) [*Mincer et al.*, 2007]. Nitrite is the intermediate form during nitrification (between ammonia and nitrate), and the nitrite maximum can be attributable to nitrification activity [*Wada and Hattori*, 1971; *Mincer et al.*, 2007; *Beman et al.*, 2008]. However, the nitrite maximum in this study did not always correspond to the maximum abundance of archaeal *amoA*, and it was more comparable to the chlorophyll *a* maximum. Nitrite is also created by phytoplankton during nitrate reduction [*Lomas and Lipschultz*, 2006]; hence, the nitrite maximum may be caused primarily by phytoplankton.

[33] We now examine the reason why archaeal *amoA* has regional differences. The relatively higher abundance of archaeal *amoA* in the ECS can be related to effective sediment resuspension on the shelf [*Matsuno et al.*, 2005, 2006]. The vertical eddy diffusivity was significantly high near the bottom of the shelf in the ECS [*Matsuno et al.*, 2005], and *Matsuno et al.* [2006] indicated that bottom waters are well ventilated. Nitrification is recognized as a major process in the nitrogen cycle in shelf sediment in the ECS [*Usui et al.*, 1998], and archaeal *amoA* is generally distributed in sediments [*Francis et al.*, 2005]. This evidence leads us to infer that a large fraction of archaeal *amoA* in the euphotic zone originates from the resuspension of shelf-bottom nitrifiers. Furthermore, *Galand et al.* [2009] recently demonstrated that horizontal transport of water masses can also play an important role in the distribution of ammonia-oxidizing archaea. Thus, the elevation of archaeal *amoA* in the deep Kuroshio, and the secondary peak at 200 m at station T0702, might actually be caused by the delivery of nitrifiers from sediments on the shelf into the Kuroshio.

4.3. Imbalance Between Nitrate Upward Flux and Nitrate Assimilation Rates

[34] Our incubation experiments potentially carried two uncertainties, either of which may have led to underestimations in nitrate assimilation. One was isotope dilution of substrate(s) caused by nitrification and excretion of fixed nitrate as DON during the incubation [*Lipschultz*, 2008]. The other was the simulation of light conditions during the onboard incubations. Light conditions were adjusted to in situ intensities using neutral-density screens, which did not simulate underwater light spectra. *Aufdenkampe et al.* [2002] compared depth-integrated nitrate assimilation in the equatorial Pacific between in situ and on-deck incubation, and found that the former gave 1.37 ± 0.09 times higher rates than

the latter. Therefore, nitrate assimilation measured during this study is a conservative estimate.

[35] At station B, a 24 h time series station in the ECS, the nitrate assimilation rate above the top of the nitracline (1500 μmolN m^{-2} d^{-1}) was one order of magnitude higher than the vertical nitrate flux (98 (52–150, 95% CI) μmolN m^{-2} d^{-1}). Regarding the depth-integrated nitrate assimilation rate, the statistical range could not be calculated because the Michaelis-Menten kinetics approach was used. However, the values obtained by the kinetics had higher accuracy than those obtained by the conventional method [*Harrison et al.*, 1996; *Kanda et al.*, 2003]. Therefore, the difference between the nitrate assimilation rate and the vertical nitrate flux is highly likely to be significant. This, in turn, indicates that other nitrate inputs to the euphotic zone, other than the diapycnal flux, existed during the observations.

[36] In the present study, archaeal *amoA* occurred at 10% light depth (50 m) at station B, which was shallower than the nitracline, while a recent study reported that the abundance of archaeal *amoA* correlated positively with ammonia oxidation rates [*Beman et al.*, 2008]. Furthermore, *Dore and Karl* [1996] reported that depth-integrated nitrification in the euphotic zone was estimated at 340–1640 μmolN m^{-2} d^{-1} at station ALOHA, in the North Pacific subtropical gyre. This estimation was similar to the range of nitrate sources for biological assimilation in the present study. Therefore, nitrate assimilation at station B can be enhanced by nitrification activity. The other possible nitrate sources are atmospheric deposition, sporadic disturbance, and advection. The ECS is located near a source of NO_x, and the atmospheric nitrate input was higher than that in the Philippine Sea [*Nakamura et al.*, 2005; *Uno et al.*, 2007]. Nitrate dry deposition in the ECS of 51 μmolN m^{-2} d^{-1} was determined by *Nakamura et al.* [2005] during their autumn cruise. Using a mathematical model, *Uno et al.* [2007] estimated that the total (dry + wet) nitrate deposition in the ECS (200–300 kgN km^{-2} yr^{-1}, equivalent to 40–60 μmolN m^{-2} d^{-1}) had no significant seasonal variations [from *Uno et al.*, 2007, Figures 2e and 3b]. Therefore, atmospheric deposition appears be insignificant as a nitrate source for the shelf. With respect to sporadic disturbances, internal waves are a possible source of nitrate during short timescales [*Holligan et al.*, 1985], though no obvious displacements of the pycnocline occurred during the observed period (data not shown). Further, the Changjiang River plume is a key nutrient source for biological production [*Chen*, 2008]. However, surface nitrate concentrations around station B were under the detection limit of the conventional method, and hence a nutrient tongue from the Changjiang River was not observed during the cruise. Nutrient advection from islands, however, might occur since station B was located near islands. Therefore, while nitrification is thought to explain the gap between nitrate assimilation and upward flux, we cannot exclude other potential sources. However, nitrification was highly likely to play an important role in nitrate-based production on the shelf.

[37] If we assume that the abundance of archaeal *amoA* is indicative of potential nitrification activity [*Beman et al.*, 2008], then the activity in the euphotic zone of the shelf is higher than that in the open ocean (Figure 6). These results might be related to the fact that the discrepancy between the vertical nitrate flux and the nitrate assimilation at station B appeared to be greater than that in the Kuroshio or the Philippine Sea (Table 1).

5. Conclusions

[38] The present study has demonstrated that the discrepancy between nitrate assimilation and diapycnal nitrate flux was large on the shelf of the ECS, with smaller discrepancies in adjacent, deep water regions of the Kuroshio and Philippine Sea. Although it is necessary to measure nitrification before a solid conclusion can be reached, according to archaeal *amoA* gene distribution, this discrepancy may be attributable in part to nitrification in the euphotic zone. Moreover, nitrification might contribute much more to nitrate-based production on the shelf than in the open ocean. Nitrification in the euphotic zone was not considered in a previous study on the biogeochemical cycle on the continental shelf [*Chen*, 2003]. Although continental shelf zones occupy only 7% of the sea surface in the world, ~14% of the total oceanic production occurs there, and important fisheries are present in this region [*Chen et al.*, 2003]. For sustainable fisheries, fish catches must be less than new production [*Eppley and Peterson*, 1979]. If nitrate-based new production has been considerably overestimated, the resource management of fisheries might have to be reassessed [*Maranger et al.*, 2008; *Qiu et al.*, 2010]. In contrast to nitrate-based new production, N_2 fixation, which is another source of new nitrogen, is recognized to have been underestimated in the oligotrophic ocean [*Karl et al.*, 1997; *Shiozaki et al.*, 2009]. To improve our basic understanding of the biogeochemical cycle on the continental shelf, it is important to reevaluate new production.

[39] **Acknowledgments.** We thank the captains, crew members, and participants on board the T/V *Nagasaki-maru* and R/V *Tansei-maru* cruises for their cooperation at sea. We acknowledge H. Ogawa, K. Hayashizaki, and M. C. Carvalho for their technical support of the mass spectrometer at Kitasato University. Thanks are also due to S. Watabe, S. Kinoshita, and H. Furuya for their suggestions during molecular experiments and to M. Sato for his suggestion on statistical analyses. Comments provided by the Associate Editor and two anonymous reviewers improved the manuscript considerably. This research was financially supported by JSPS grants 14658151, 17651003, 18067006, and 19030005.

References

Aufdenkampe, A. K., J. J. McCarthy, C. Navarette, M. Rodier, J. Dunne, and J. W. Murray (2002), Biogeochemical controls on new production in the tropical Pacific, *Deep Sea Res., Part II*, *49*, 2619–2648, doi:10.1016/S0967-0645(02)00051-6.

Beman, J. M., B. N. Popp, and C. A. Francis (2008), Molecular and biogeochemical evidence for ammonia oxidation by marine Crenarchaeota in the Gulf of California, *ISME J.*, *2*, 429–441, doi:10.1038/ismej.2007.118.

Carr, M. E., M. R. Lewis, D. Kelley, and B. Jones (1995), A physical estimate of new production in the equatorial Pacific along 150°W, *Limnol. Oceanogr.*, *40*, 138–147, doi:10.4319/lo.1995.40.1.0138.

Chen, C. T. A. (2003), New vs. export production on the continental shelf, *Deep Sea Res., Part II*, *50*, 1327–1333, doi:10.1016/S0967-0645(03)00026-2.

Chen, C. T. A. (2008), Distribution of nutrients in the East China Sea and the South China Sea connection, *J. Oceanogr.*, *64*, 737–751, doi:10.1007/s10872-008-0062-9.

Chen, C. T. A., K. K. Liu, and R. MacDonald (2003), Continental margin exchanges, in *Ocean Biogeochemistry*, edited by M. J. R. Fasham, pp. 53–97, Springer, New York.

Chen, Y.-L. L., H. B. Lu, F. K. Shiah, G. C. Gong, K. K. Liu, and J. Kanda (1999), New production and F-ratio on the continental shelf of the East China Sea: Comparisons between nitrate inputs from the subsurface

Kuroshio current and the Changjian River, *Estuarine Coastal Shelf Sci.*, *48*, 59–75, doi:10.1006/ecss.1999.0404.

Chen, Y.-L. L., H. Y. Chen, W. H. Lee, C. C. Hung, G. T. F. Wong, and J. Kanda (2001), New production in the East China Sea, comparison between well-mixed winter and stratified summer conditions, *Cont. Shelf Res.*, *21*, 751–764, doi:10.1016/S0278-4343(00)00108-4.

Clark, D. R., A. P. Rees, and I. Joint (2008), Ammonium regeneration and nitrification rates in the oligotrophic Atlantic Ocean: Implications for new production estimates, *Limnol. Oceanogr.*, *53*, 52–62, doi:10.4319/lo.2008.53.1.0052.

Dore, J. E., and D. M. Karl (1996), Nitrification in the euphotic zone as a source for nitrite, nitrate and nitrous oxide at Station ALOHA, *Limnol. Oceanogr.*, *41*, 1619–1628, doi:10.4319/lo.1996.41.8.1619.

Dugdale, R. C., and J. J. Goering (1967), Uptake of new and regenerated forms of nitrogen in primary productivity, *Limnol. Oceanogr.*, *12*, 196–206, doi:10.4319/lo.1967.12.2.0196.

Efron, A., and G. Gong (1983), A leisurely look at the bootstrap, the jackknife and cross-validation, *Am. Stat.*, *37*, 36–48, doi:10.2307/2685844.

Eppley, R. W., and B. J. Peterson (1979), Particulate organic matter flux and planktonic new production in the deep ocean, *Nature*, *282*, 677–680, doi:10.1038/282677a0.

Francis, C. A., K. J. Roberts, J. M. Beman, A. E. Santoro, and B. B. Oakley (2005), Ubiquity and diversity of ammonia-oxidizing archaea in water columns and sediments of the ocean, *Proc. Natl. Acad. Sci. U. S. A.*, *102*, 14,683–14,688, doi:10.1073/pnas.0506625102.

Galand, P. E., C. Lovejoy, A. K. Hamilton, R. G. Ingram, E. Pedneault, and E. C. Carmack (2009), Archaeal diversity and a gene for ammonia oxidation are coupled to oceanic circulation, *Environ. Microbiol.*, *11*, 971–980, doi:10.1111/j.1462-2920.2008.01822.x.

Harrison, W. G., L. R. Harris, and B. D. Irwin (1996), The kinetics of nitrogen utilization in the oceanic mixed layer: Nitrate and ammonium interactions at nanomolar concentrations, *Limnol. Oceanogr.*, *41*, 16–32, doi:10.4319/lo.1996.41.1.0016.

Hashihama, F., K. Furuya, S. Kitajima, S. Takeda, T. Takemura, and J. Kanda (2009), Macro-scale exhaustion of surface phosphate by dinitrogen fixation in the western North Pacific, *Geophys. Res. Lett.*, *36*, L03610, doi:10.1029/2008GL036866.

Holligan, P. M., R. D. Pingree, and G. T. Mardell (1985), Oceanic solitons, nutrient pulses and phytoplankton growth, *Nature*, *314*, 348–350, doi:10.1038/314348a0.

Kanda, J., T. Itoh, D. Ishizaka, and Y. Watanabe (2003), Environmental controls of nitrate uptake in the East China Sea, *Deep Sea Res., Part II*, *50*, 403–422, doi:10.1016/S0967-0645(02)00464-2.

Karl, D., R. Letelier, L. Tupas, J. Dore, J. Christian, and D. Hebel (1997), The role of nitrogen fixation in biogeochemical cycling in the subtropical North Pacific Ocean, *Nature*, *388*, 533–538, doi:10.1038/41474.

King, F. D., and A. H. Devol (1979), Estimates of vertical eddy diffusion through the thermocline from phytoplankton nitrate uptake rates in the mixed layer of the eastern tropical Pacific, *Limnol. Oceanogr.*, *24*, 645–651, doi:10.4319/lo.1979.24.4.0645.

Lewis, M. R., W. G. Harrison, N. S. Oakey, D. Hebert, and T. Platt (1986), Vertical nitrate fluxes in the oligotrophic ocean, *Science*, *234*, 870–873, doi:10.1126/science.234.4778.870.

Lipschultz, F. (2008), Isotope tracer methods for studies of the marine nitrogen cycle, in *Nitrogen in the Marine Environment*, 2nd ed., edited by D. G. Capone et al., pp. 1345–1384, Academic, Burlington Mass., doi:10.1016/B978-0-12-372522-6.00031-1.

Lomas, M. W., and F. Lipschultz (2006), Forming the primary nitrite maximum: Nitrifiers or phytoplankton?, *Limnol. Oceanogr.*, *51*, 2453–2467, doi:10.4319/lo.2006.51.5.2453.

Maranger, R., N. Caraco, J. Duhamel, and M. Amyot (2008), Nitrogen transfer from sea to land via commercial fisheries, *Nat. Geosci.*, *1*, 111–112, doi:10.1038/ngeo108.

Matsuno, T., M. Shimizu, Y. Morii, H. Nishida, and Y. Takaki (2005), Measurements of the turbulent energy dissipation rate around the shelf break in the East China Sea, *J. Oceanogr.*, *61*, 1029–1037, doi:10.1007/s10872-006-0019-9.

Matsuno, T., J.-S. Lee, M. Shimizu, S.-H. Kim, and I.-C. Pang (2006), Measurements of the turbulent energy dissipation rate and an evaluation of the dispersion process of the Changjiang Diluted Water in the East China Sea, *J. Geophys. Res.*, *111*, C11S09, doi:10.1029/2005JC003196.

Mincer, T. J., M. J. Church, L. T. Taylor, C. Preston, D. M. Karl, and E. F. DeLong (2007), Quantitative distribution of presumptive archaeal and bacterial nitrifiers in Monterey Bay and the North Pacific Subtropical Gyre, *Environ. Microbiol.*, *9*, 1162–1175, doi:10.1111/j.1462-2920.2007.01239.x.

Nakamura, T., K. Matsumoto, and M. Uematsu (2005), Chemical characteristics of aerosols transported from Asia to the East China Sea: An evaluation of anthropogenic combined nitrogen deposition in autumn, *Atmos. Environ.*, *39*, 1749–1758.

Osborn, T. R. (1980), Estimates of the local rate of vertical diffusion from dissipation measurements, *J. Phys. Oceanogr.*, *10*, 83–89, doi:10.1175/1520-0485(1980)010<0083:EOTLRO>2.0.CO;2.

Peña, M. A., W. G. Harrison, and M. R. Lewis (1992), New production in the central equatorial Pacific, *Mar. Ecol. Prog. Ser.*, *80*, 265–274, doi:10.3354/meps080265.

Qiu, Y., Z. Lin, and Y. Wang (2010), Responses of fish production to fishing and climate variability in the northern South China Sea, *Prog. Oceanogr.*, *85*, 197–212, doi:10.1016/j.pocean.2010.02.011.

Shiozaki, T., K. Furuya, T. Kodama, and S. Takeda (2009), Contribution of N_2 fixation to new production in the western North Pacific Ocean along 155°E, *Mar. Ecol. Prog. Ser.*, *377*, 19–32, doi:10.3354/meps07837.

Shiozaki, T., K. Furuya, T. Kodama, S. Kitajima, S. Takeda, T. Takemura, and J. Kanda (2010), New estimation of N_2 fixation in the western and central Pacific Ocean and its marginal seas, *Global Biogeochem. Cycles*, *24*, GB1015, doi:10.1029/2009GB003620.

Siswanto, E., J. Ishizaka, and K. Yokouchi (2005), Estimating chlorophyll-*a* vertical profiles from satellite data and implication for primary production in the Kuroshio front of the East China Sea, *J. Oceanogr.*, *61*, 575–589, doi:10.1007/s10872-005-0066-7.

Suzuki, R., and T. Ishimaru (1990), An improved method for the determination of phytoplankton chlorophyll using N,N-dimethylformamide, *J. Oceanogr. Soc. Jpn.*, *46*, 190–194, doi:10.1007/BF02125580.

Tillett, D., and B. A. Neilan (2000), Xanthogenate nucleic acid isolation from cultured and environmental cyanobacteria, *J. Phycol.*, *36*, 251–258, doi:10.1046/j.1529-8817.2000.99079.x.

United Nations Educational, Scientific and Cultural Organization (UNESCO) (1994), *Protocols for the Joint Global Ocean Flux Study (JGOFS) Core Measurements*, *IOC Manuals and Guides*, no. 29, pp. 145–150, Paris.

Uno, I., M. Uematsu, Y. Hara, Y. J. He, T. Ohara, A. Mori, T. Kamaya, K. Murano, Y. Sadanaga, and H. Bandow (2007), Numerical study of the atmospheric input of anthropogenic total nitrate to the marginal seas in the western North Pacific region, *Geophys. Res. Lett.*, *34*, L17817, doi:10.1029/2007GL030338.

Usui, T., I. Koike, and N. Ogura (1998), Vertical profiles of nitrous oxide and dissolved oxygen in marine sediments, *Mar. Chem.*, *59*, 253–270, doi:10.1016/S0304-4203(97)00091-1.

Wada, E., and A. Hattori (1971), Nitrite metabolism in the euphotic layer of the central North Pacific Ocean, *Limnol. Oceanogr.*, *16*, 766–772, doi:10.4319/lo.1971.16.5.0766.

Wada, E., and A. Hattori (1991), *Nitrogen in the Sea: Forms, Abundances, and Rate Processes*, CRC Press, Boca Raton, Fla.

Wuchter, C., et al. (2006), Archaeal nitrification in the ocean, *Proc. Natl. Acad. Sci. U. S. A.*, *103*, 12,317–12,322, doi:10.1073/pnas.0600756103.

Yool, A., A. P. Martin, C. Fernández, and D. R. Clark (2007), The significance of nitrification for oceanic new production, *Nature*, *447*, 999–1002, doi:10.1038/nature05885.

T. Endoh, T. Matsuno, and Y. Yoshikawa, Research Institute for Applied Mechanics, Kyushu University, Kasuga, Fukuoka 816-8580, Japan.

K. Furuya, T. Kodama, and T. Shiozaki, Department of Aquatic Bioscience, Graduate School of Agricultural and Life Sciences, University of Tokyo, 1-1-1 Yayoi, Bunkyo-ku, Tokyo 113-8657, Japan. (furuya@fs.a.u-tokyo.ac.jp)

J. Ishizaka, Hydrospheric Atmospheric Research Center, Nagoya University, Furo-cho, Chikusa-ku, Nagoya 464-8601, Japan.

H. Kurotori, Riso Co. Ltd., 1-36-1, Yoyogi, Shibuya, Tokyo 151-0053, Japan.

S. Takeda, Graduate School of Fisheries Science and Environmental Studies, Nagasaki University, Bunkyo, Nagasaki 852-8521, Japan.